Robust Signal Processing for Damaged Vehicles with Uncertainty

Sung-Kwon Hong

Department of Mechanical Engineering, University of Michigan,
2350 Hayward Street, Ann Arbor, Michigan 48109-2125, U.S.A.
E-mail: sungkwon@umich.edu

Bogdan I. Epureanu*

Department of Mechanical Engineering, University of Michigan,
2350 Hayward Street, Ann Arbor, Michigan 48109-2125, U.S.A.
E-mail: epureanu@umich.edu
*Corresponding author

Matthew P. Castanier

U.S. Army Tank Automotive Research, Development, and
Engineering Center,
Warren, MI 48397-5000, U.S.A.
E-mail: matt.castanier@us.army.mil

Abstract: The focus of this paper is on establishing a robust signal processing approach for damaged vehicles (i.e., cracked structures) with geometric and material uncertainties such as thicknesses of various components and Young's modulus variations. The approach assumes that vibration-type data is collected during the operation of a vehicle. Next, the collected data is used in a novel combined sensor selection and signal processing methodology. The new methodology resolves two key issues for complex structures with uncertainty: (1) decides which field data channels are statistically optimal to be used, and (2) establishes which data channels should correlate and how. The overall algorithm is based on a generalized version of the effective independence distribution vector. Also, the correlations among channels are used for noise rejection. Furthermore, the dynamics of the vehicle (i.e., a complex structure with uncertainties) is modeled using parametric reduced order models (PROMs) and the concept of bilinear mode shapes introduced recently by the authors for cracked structures. PROMs are used to address the presence of uncertainty and account for their effects on the data collected from various channels. The bilinear modes are used to capture the effects of the crack. The proposed methodology is demonstrated for a complex/realistic model of a HMMWV frame with parameter variations/uncertainty and a crack.

Keywords: robust signal processing; uncertainties; parametric reduced order models (PROMs); effective independence distribution vector; bilinear mode shapes.

Report Documentation Page

Form Approved
OMB No. 0704-0188

1. REPORT DATE	2. REPORT TYPE	3. DATES COVERED
23 FEB 2011	**N/A**	**-**

4. TITLE AND SUBTITLE	5a. CONTRACT NUMBER
Robust Signal Processing for Damaged Vehicles with Uncertainty (PREPRINT)	5b. GRANT NUMBER
	5c. PROGRAM ELEMENT NUMBER
6. AUTHOR(S)	5d. PROJECT NUMBER
Sung-Kwon Hong; Bogdan I. Epureanu; Matthew P. Castanier	5e. TASK NUMBER
	5f. WORK UNIT NUMBER
7. PERFORMING ORGANIZATION NAME(S) AND ADDRESS(ES)	8. PERFORMING ORGANIZATION REPORT NUMBER
US Army RDECOM-TARDEC 6501 E 11 Mile Rd Warren, MI 48397-5000, USA Department of Mechanical Engineering, University of Michigan, 2350 Hayward Street, Ann Arbor, Michigan 48109-2125, U.S.A.	**21555**
9. SPONSORING/MONITORING AGENCY NAME(S) AND ADDRESS(ES)	10. SPONSOR/MONITOR'S ACRONYM(S)
US Army RDECOM-TARDEC 6501 E 11 Mile Rd Warren, MI 48397-5000, USA	**TACOM/TARDEC/RDECOM**
	11. SPONSOR/MONITOR'S REPORT NUMBER(S) **21555**

12. DISTRIBUTION/AVAILABILITY STATEMENT
Approved for public release, distribution unlimited

13. SUPPLEMENTARY NOTES
Submitted for publication in a Special Issue of Int'l Journal of Vehicle Design, The original document contains color images.

14. ABSTRACT
The focus of this paper is on establishing a robust signal processing approach for damaged vehicles (i.e., cracked structures) with geometric and material uncertainties such as thicknesses of various components and Youngs modulus variations. The approach assumes that vibration-type data is collected during the operation of a vehicle. Next, the collected data is used in a novel combined sensor selection and signal processing methodology. The new methodology resolves two key issues for complex structures with uncertainty: (1) decides which field data channels are statistically optimal to be used, and (2) establishes which data channels should correlate and how. The overall algorithm is based on a generalized version of the effective independence distribution vector. Also, the correlations among channels are used for noise rejection. Furthermore, the dynamics of the vehicle (i.e., a complex structure with uncertainties) is modeled using parametric reduced order models (PROMs) and the concept of bilinear mode shapes introduced recently by the authors for cracked structures. PROMs are used to address the presence of uncertainty and account for their effects on the data collected from various channels. The bilinear modes are used to capture the effects of the crack. The proposed methodology is demonstrated for a complex/realistic model of a HMMWV frame with parameter variations/uncertainty and a crack.

15. SUBJECT TERMS					
robust signal processing; uncertainties; parametric reduced order models (PROMs); effective independence distribution vector; bilinear mode shapes					
16. SECURITY CLASSIFICATION OF:			17. LIMITATION OF ABSTRACT	18. NUMBER OF PAGES	19a. NAME OF RESPONSIBLE PERSON
a. REPORT	b. ABSTRACT	c. THIS PAGE			
unclassified	**unclassified**	**unclassified**	**SAR**	**21**	

Standard Form 298 (Rev. 8-98)
Prescribed by ANSI Std Z39-18

1 Introduction

Vibration-based structural health monitoring (SHM) techniques are of current interest in identifying damage and assessing the integrity of structures such as ground vehicles. Predicting the dynamic characteristics of damaged structures is an important challenge for vibration-based SHM. The numbers of degrees of freedom (DOFs) of the finite element models used to predict the dynamic response of complex structures are prohibitively large, so conventional finite element analysis are hard to employ. Thus, alternative techniques have been developed recently to predict the dynamic response of complex structures with models having a dramatically lower number of DOFs (Hurty (1965); Craig and Bampton (1968); Rubin (1975); Hintz (1975); Craig and Chang (1976)). These reduced-order models (ROMs) are increasingly used to predict the vibration response of the structures, especially their resonant frequencies and mode shapes, using a short computational time and a low computational cost. One method for constructing ROMs is based on the fixed-interface component mode synthesis (CB-CMS) (Craig and Bampton (1968)). That well known approach is employed herein for a few portions of the model. Specifically, CB-CMS is useful and applied only to the invariant components of overall/entire structures. A component is considered invariant if it does not have any geometrical or structural variations. However, for the vibration-based SHM, the challenge is to predict the vibration characteristics of damaged structures, not those of pristine structures. If one attempts to use standard reduced order modeling techniques when parametric changes (such as thickness and geometrical variations) are applied by design or exist through damage, the finite element model has to be modified, and new ROMs have to be reconstructed (through a reanalysis) to predict the structural vibration response. That is a manual and a very costly process computationally. Recently, design oriented ROMs have been developed to avoid such prohibitively expensive reanalyses of complex structures. These models are parametric reduced order models (PROMs). Initially, global PROMs have been developed (see e.g. the work of Balmes (1996); Balmes, et al. (2004)). However, global PROMs are impractical because they require one to repeatedly solve many sample eigenproblems for the entire structure. Thus, component-mode-based PROMs (Zhang, et al. (2005)) have been developed to adopt component normal modes and characteristic constraint modes as projection basis instead of global modes. However, constructing component-mode-based PROMs as done in Zhang, et al. (2005) is also time consuming because the approach still requires the calculation of system-level (global) interface modes. Thus, Park (2008) introduced truly component-level analysis for constructing PROMs, referred to as component-PROMs. However, in their approach, component-PROMs can be applied only to one component. Thus, the multiple-component PROMs (MC-PROMs) have been developed by the authors (Hong, et al. (2010)) and are adopted herein to allow complex structures to be divided into several, much simpler, substructures. Each substructure can have variability in characteristics such as geometric parameters (e.g. thickness) or material properties (e.g. Young's modulus).

In this work, PROM techniques employing CB-CMS and MC-PROM are applied to analyze the vibration response of a cracked complex structure. Also, note that the

cracked structure generates a nonlinear dynamic problem because of the nonlinear contact force between the crack surfaces. One approach to handle this nonlinear contact force is to use a hybrid frequency-time domain (HFT) method developed by Poudou and Pierre (2003), Poudou (2004), and Saito, et al. (2009). In that method, a forced response analysis is applied to determine the resonant frequencies of the cracked structure. While powerful, that approach is computationally intensive, and difficult to use to predict resonant responses (due to the nonlinearity). Thus, an alternate approach (based on linear analyses) has been developed for predicting resonant frequencies. The alternate approach builds on earlier work on the bilinear frequency approximation (BFA) (Chati, et al. (1997)). The resonant frequencies predicted by the generalized BFA have been shown to agree very well with those obtained using nonlinear HFT analyses for applications such as cracked turbine bladed disks (Saito, et al. (2009)). Herein, the concept of BFA is adopted together with the bilinear mode approximation (BMA) (Saito and Epureanu (2010)). BMA is introduced to approximate the mode shapes of cracked structures. In addition, to reduce computational cost for BMA, PROM techniques based on CB-CMS and MC-PROMs are used.

The characteristics of the dynamic response obtained using PROMs technique are useful signals for vibration-based SHM. However, all signals obtained from PROM cannot be used in practice due to limited accessibility constraints and cost of the needed sensors. Thus, robust signal processing techniques to find the best sensor locations are an important challenge. There are many previous studies of sensor placement for SHM. For example, Ansari (2007) has implemented SHM strategies which require selection and placement of sensors suitable for measuring key parameters that influence the performance and health of civil structures. Flynn, et al. (2009) have proposed a novel approach for optimal actuator and sensor placement for SHM. Krommer, et al. (2009) have investigated a sensor network composed of strain-type patch sensors with constant intensity designed to replace distributed strain-type sensors for monitoring beam-type structures. Herein, a novel robust signal processing technique is employed to find the optimal number of sensor locations for gathering mode shape information of cracked structures. The novel approach is developed starting from an algorithm based on the effective independence distribution vector (EIDV) (Kammer (1991); Penny, et al. (1994)). The key idea of EIDV is to choose sensor locations for measuring physical mode shapes as linearly independent as possible in the frequency range of interest. Herein, the EIDV method is modified to select optimal sensor locations for cracked complex structures. The number of selected locations based on the modified EIDV method is not only limited to the frequency range of interest, but also limited in the effects of measurement noise. To address this noise, over-sampling is often performed. EIDV cannot provide optimal locations for over-sampling. Herein, a new signal processing technique is developed to select over-sampled measurement locations.

To approximate the mode shapes of cracked structures, BMA is formulated based on PROM mode shapes. For completeness, this paper briefly describes also the PROMs approach to construct models for structures with parametric variabilities. Finally, robust signal processing techniques are proposed to select the optimal and minimal sensor locations to capture the mode shapes of the structures. The technique to find optimal sensor locations is specifically designed for cases where the structure has structural variability and a crack.

2 Bilinear Mode Approximation

In this section, the mode shapes of a structure with a crack of various lengths are examined. When a structure has a crack, the resonant responses are hard to compute due to the nonlinearity of dynamics. This dynamics is caused by the periodic opening and closing of the crack surface (which leads to a piece-wise linear dynamics). Hence, to predict the mode shapes, standard modal analyses cannot be directly employed. To address this challenge, a novel technique to characterize the spatial correlations among the vibration of various points within the structure has been developed. These correlations are akin to mode shapes, but they characterize the dynamics of the cracked (nonlinear) structure. This approach is based on the observation that, when the structure has a crack and vibrates at some (nonlinear) resonant frequency, two states can be identified: crack open and crack closed. These two states correspond to two shapes for the deformation of the structure at that frequency. Next, we assume that all the shapes the structure takes during its nonlinear vibration at a resonant frequency are linear combinations of these two shapes (open and closed at that resonant frequency). Furthermore, the open and closed shapes are assumed to be very similar to the shapes the structure would have if the crack surface were permanently open (i.e., penetration would be allowed) or permanently closed (with sliding occurring between DOFs within the crack surface). These linear modes can be easily computed by standard linear techniques. This novel approach is referred to as BMA, and complements BFA (Chati, et al. (1997)) originally developed for discrete low-dimensional systems and later generalized for cracked structures. The bilinear (BL) modes $\mathbf{\Phi}_{\mathrm{BL}}$ can be expressed as

$$\mathbf{\Phi}_{\mathrm{BL}} = \begin{bmatrix} \mathbf{\Phi}_{\mathrm{open}} \\ \mathbf{\Phi}_{\mathrm{closed}} \end{bmatrix}, \tag{1}$$

where $\mathbf{\Phi}_{\mathrm{open}}$ are the mode shapes of the structure with a permanently open crack (penetration allowed) and $\mathbf{\Phi}_{\mathrm{closed}}$ are the mode shapes of the structure with a permanently closed crack (sliding allowed).

3 Parametric Reduced Order Models

In this section, the well known fixed-interface Craig-Bampton CMS (CB-CMS) method (Craig and Bampton (1968)) and multiple-component parametric reduced-order models (MC-PROM) (Hong, et al. (2010)) used to construct PROMs for healthy substructures and substructures with parameter variations are briefly reviewed.

First, the CB-CMS approach (Craig and Bampton (1968)) is used to model only the substructures which do not have any structural variability. This modeling approach is used because it is very simple and computationally stable. Also, this technique is derivable because it can be exploited when modeling cracked structures by managing the geometric compatibility conditions between substructures. To apply CB-CMS, the complex structure of interest is partitioned into substructures, and the substructures have interface DOF and internal DOFs. The physical coordinates of these interface and internal DOFs are projected onto the generalized coordinates by using the fixed-interface normal mode ($\mathbf{\Phi}_{\mathbf{i}}^{\mathbf{N}}$) and static constraint mode ($\mathbf{\Psi}_{\mathbf{i}}^{\mathbf{C}}$). Then, the size of the mass and stiffness matrices, and force vector for substructure i are significantly reduced.

Second, MC-PROMs (Hong, et al. (2010)) are adopted to manage the substructures with variability in parameters such as Young's modulus and thickness variations. One important advantage of MC-PROMs is that the finite element mesh of the nominal structure does not need to be modified, although the substructures have parametric variability. That is because the mass and stiffness matrices are parameterized (by using Taylor series). For example, for a linear thin plate element, the modification of the stiffness matrix due to variations in the thickness of the plate can be accurately represented by a Taylor series up to third order within an upper and a lower limit for the parameterization. In addition, similar to the CB-CMS, an appropriate transformation matrix is constructed for converting from physical coordinates to generalized coordinates by using fixed-interface normal modes and static constraint modes. The distinct feature between CB-CMS and MC-PROM is that the transformation matrix for MC-PROM is constructed for all configurations in the parameter space of the corresponding component. In contrast, CB-CMS applied only to components with no parameter variability.

The i^{th} and j^{th} component mass and stiffness matrices for CB-CMS and MC-PROM are partitioned as Hong, et al. (2010) and are explained as

$$\mathbf{M}_i^{CMS} = \begin{bmatrix} \mathbf{m}_i^{CC} & \mathbf{m}_i^{CF} & \mathbf{m}_i^{CCN} \\ \mathbf{m}_i^{FC} & \mathbf{m}_i^{FF} & \mathbf{m}_i^{FFN} \\ \mathbf{m}_i^{NCC} & \mathbf{m}_i^{NFF} & \mathbf{m}_i^{NN} \end{bmatrix}, \quad \hat{\mathbf{K}}_i^{CMS} = \begin{bmatrix} \mathbf{k}_i^{CC} & \mathbf{k}_i^{CF} & \mathbf{k}_i^{CCN} \\ \mathbf{k}_i^{FC} & \mathbf{k}_i^{FF} & \mathbf{k}_i^{FFN} \\ \mathbf{k}_i^{NCC} & \mathbf{k}_i^{NFF} & \mathbf{k}_i^{NN} \end{bmatrix}, \quad (2)$$

$$\begin{aligned} \mathbf{M}_j^{PROM} &= \begin{bmatrix} \mathbf{m}_j^{CC_{00}} & \mathbf{m}_j^{CF_{00}} & \mathbf{m}_j^{CC_{0U}} & \mathbf{m}_j^{CF_{0U}} & \mathbf{m}_j^{CCN_{00}} \\ \mathbf{m}_j^{FC_{00}} & \mathbf{m}_j^{FF_{00}} & \mathbf{m}_j^{FC_{0U}} & \mathbf{m}_j^{FF_{0U}} & \mathbf{m}_j^{FFN_{00}} \\ \mathbf{m}_j^{CC_{U0}} & \mathbf{m}_j^{CF_{U0}} & \mathbf{m}_j^{CC_{UU}} & \mathbf{m}_j^{CF_{UU}} & \mathbf{m}_j^{CCN_{UU}} \\ \mathbf{m}_j^{FC_{U0}} & \mathbf{m}_j^{FF_{U0}} & \mathbf{m}_j^{FC_{UU}} & \mathbf{m}_j^{FF_{UU}} & \mathbf{m}_j^{FFN_{UU}} \\ \mathbf{m}_j^{NCC_{00}} & \mathbf{m}_j^{NFF_{00}} & \mathbf{m}_j^{NCC_{UU}} & \mathbf{m}_j^{NFF_{UU}} & \mathbf{m}_j^{N_d} \end{bmatrix}, \\ \mathbf{K}_j^{PROM} &= \begin{bmatrix} \mathbf{k}_j^{CC_{00}} & \mathbf{k}_j^{CF_{00}} & \mathbf{k}_j^{CC_{0U}} & \mathbf{k}_j^{CF_{0U}} & \mathbf{k}_j^{CCN_{00}} \\ \mathbf{k}_j^{FC_{00}} & \mathbf{k}_j^{FF_{00}} & \mathbf{k}_j^{FC_{0U}} & \mathbf{k}_j^{FF_{0U}} & \mathbf{k}_j^{FFN_{00}} \\ \mathbf{k}_j^{CC_{U0}} & \mathbf{k}_j^{CF_{U0}} & \mathbf{k}_j^{CC_{UU}} & \mathbf{k}_j^{CF_{UU}} & \mathbf{k}_j^{CCN_{UU}} \\ \mathbf{k}_j^{FC_{U0}} & \mathbf{k}_j^{FF_{U0}} & \mathbf{k}_j^{FC_{UU}} & \mathbf{k}_j^{FF_{UU}} & \mathbf{k}_j^{FFN_{UU}} \\ \mathbf{k}_j^{NCC_{00}} & \mathbf{k}_j^{NFF_{00}} & \mathbf{k}_j^{NCC_{UU}} & \mathbf{k}_j^{NFF_{UU}} & \mathbf{k}_j^{N_d} \end{bmatrix}, \end{aligned} \quad (3)$$

where the superscript 0 indicates the nominal parameter values, and the superscript U indicate quantities computed for the upper limit parameter values in Eq. (3).

To model the dynamics of cracked structures and to apply BMA, the partitioning of the structure is done such that all crack surfaces are along interfaces between adjacent substructures. That way, the crack model can be obtained by simply managing the geometric compatibility conditions. In Eqs. (2) and (3), the interface DOFs are divided into constraint DOFs (superscript CC) and free DOFs (superscript FF). For the open crack case, the DOFs between the crack surfaces are completely free, which means that those DOFs are allowed to inter-penetrate. These DOFs on the crack surfaces are free DOF (superscript FF) in Eqs. (2) and (3). For the closed crack case, sliding boundary conditions are applied at the DOFs on the crack surfaces. Hence, the DOFs on the crack interface can slide, but they are not allowed to inter-penetrate. The constrained DOFs

which are not allowed to inter-penetrate are denoted by superscript CC in Eqs. (2) and (3). The constrained (CC) and the free (FF) DOFs for the open and closed states of the cracked structure are different between shell-type and solid-type finite elements. That is because the DOFs of a nodal point are different between shell and solid-type finite elements. Thus, the DOF which are constrained (CC) or free (FF) for open and close state should be chosen carefully for each type of finite element. Using these two kinds of geometric compatibility conditions, the mode shapes of a cracked structure with an open crack and separately a closed crack are obtained through two separate linear analyses. Note also that, if component i has a crack surface, the component-level mass and stiffness matrices are partitioned as in Hong, et al. (2010).

Since all crack surfaces are at interfaces between components, all boundary DOFs are active DOFs. Finally, the geometric compatibility conditions used to assemble every substructure are applied only to the DOFs marked as CC in Eq. (2). The detailed formulation and description of PROMs technique are provided in Hong, et al. (2010).

4 Signal Processing for Cracked Structures

The objective of the signal processing technique is to select optimal sensor locations to represent the mode shapes of structures with various crack lengths. These mode shapes are useful in vibration-based SHM. An important related challenge is how to determine the frequency range of interest together with the sensor locations as to capture the shapes of the cracked structure during its vibration. Thus, a methodology to determine the sensitive modes due to the crack is investigated first.

4.1 Generalized Modal Assurance Criterion

Some of the shapes of the resonant response of the healthy structure are similar to those of the cracked structure, and some are different. For instance, when the structure has a small crack, the mode shapes of the healthy structure are very similar to those of the cracked structure. Such a resonant response is not good for detecting the location and size of the crack. To address that, the most sensitive bilinear (BL) modes are used. To identify these BL modes, a modal assurance criterion (MAC) (Allemang and Brown (1982); Allemang (2003)) has been generalized and used to obtain the $\mathbf{MAC}$ matrix between the BL modes for the healthy and the cracked structures. The new $\mathbf{MAC}$ matrix needs the BL mass matrix obtained separately using ROMs for the open and closed crack vibration cases because the BL mode shapes for the open and closed states are mass normalized, and their sizes are different due to the distinct geometric compatibility conditions. The BL mass matrix can be expressed as

$$\mathbf{M}_{\mathrm{BL}} = \begin{bmatrix} \mathbf{M}_{\mathrm{ROM}}^{\mathrm{open}} & \mathbf{0} \\ \mathbf{0} & \mathbf{M}_{\mathrm{ROM}}^{\mathrm{closed}} \end{bmatrix}, \tag{4}$$

where the two mass matrices for open and closed states are obtained from ROMs. Herein, ROMs are obtained by using CB-CMS and MC-PROMs. This BL mass matrix is used together with the BL modes to define a new MAC as

$$\mathbf{MAC}_{ij} = \frac{[(\mathbf{\Phi}_{\mathrm{BL,i}}^{\mathrm{h}})^{\mathrm{T}}\mathbf{M}_{\mathrm{BL}}(\mathbf{\Phi}_{\mathrm{BL,j}}^{\mathrm{d}})]^2}{[(\mathbf{\Phi}_{\mathrm{BL,i}}^{\mathrm{h}})^{\mathrm{T}}\mathbf{M}_{\mathrm{BL}}(\mathbf{\Phi}_{\mathrm{BL,i}}^{\mathrm{h}})][(\mathbf{\Phi}_{\mathrm{BL,j}}^{\mathrm{d}})^{\mathrm{T}}\mathbf{M}_{\mathrm{BL}}(\mathbf{\Phi}_{\mathrm{BL,j}}^{\mathrm{d}})]}, \tag{5}$$

where the subscripts i and j indicate the i^{th} and j^{th} modes, and the BL mode shapes for the healthy structure (indicated by the superscript h) are defined as in Eq. (1) but for a zero crack length, while the BL modes for a non-zero crack are indicated by the superscript d. The value $\mathbf{MAC}_{ij}$ reflects how distinct is the i^{th} BL mode of the healthy structure from the j^{th} BL mode of the cracked structure. Note that the $\mathbf{MAC}$ matrix can be computed for structures with different crack lengths. The (diagonal) entries that correspond to non-sensitive BL modes are close to 1.0 because the BL modes are normalized by the BL mass matrix. A specific example of selecting sensitive modes is showed in the next sections.

4.2 Modified Effective Independence Distribution Vector (EIDV) Algorithm

In a practical implementation for structural inspection or damage identification, information of the BL modes has to be obtained through measurements by using sensors. To address that challenge, a signal processing algorithm for selecting the minimal and optimal locations to be measured or instrumented with sensors has been developed. This algorithm is generalized from a derivative of the EIDV method (Penny, et al. (1994)). Generally, the EIDV method requires only a portion of the modal matrix of a structure in a frequency range of interest. This portion is allocated based on the generalized MAC discussed in the previous section and is applied to the BL modes and not the usual linear modes. The portion indicates also that the modal matrix has information of a set of candidate DOFs, not all DOF of the structure. The partial modal matrix is used to compute a Fisher (information) matrix which, in turn, allows the computation of an effective independence distribution vector. This vector identifies the DOFs that are best to measure in terms of ensuring the linear independence of the measurements. To apply EIDV, the augmented bilinear modal matrix $\mathbf{\Phi}_{\text{aug}}^{\text{EIDV}}$ of the cracked structure is used instead of real nonlinear mode shapes of the cracked structure. $\mathbf{\Phi}_{\text{aug}}^{\text{EIDV}}$ is formed by grouping BL modes for the healthy structure (without a crack) $\hat{\mathbf{\Phi}}_{\text{BL}}^{\text{h}}$ and the BL modes for cracked structures with various crack lengths. The matrix $\hat{\mathbf{\Phi}}_{\text{BL}}^{\text{h}}$ and all mode shapes of various cracked structures are assembled in the frequency range of interest as follows

$$\mathbf{\Phi}_{\text{aug}}^{\text{EIDV}} = [\ \hat{\mathbf{\Phi}}_{\text{BL}}^{\text{h}}\ \ \hat{\mathbf{\Phi}}_{\text{BL}}^{a\%}\ \ \hat{\mathbf{\Phi}}_{\text{BL}}^{b\%}\ \ \cdots\ ], \tag{6}$$

where $\hat{\mathbf{\Phi}}_{\text{BL}}^{a\%}$ and $\hat{\mathbf{\Phi}}_{\text{BL}}^{b\%}$ indicate the modal matrices of cracked structures with a crack length of $a\%$ and $b\%$ of a reference length. This reference length can be interpreted as the largest crack length of interest. Also, each modal matrix for the cracked structures can correspond to different frequency ranges because the sensitive modes can be different for each crack length. For instance, if the sensitive mode shapes based on $\mathbf{MAC}$ are 3^{rd}, 4^{th} and 5^{th} for the cracked structure with $a\%$ crack length, then the $\hat{\mathbf{\Phi}}_{\text{BL}}^{a\%}$ modal matrix has only three coherences with candidate DOFs. However, the sensitive modes for the cracked structure with $b\%$ can be different and can contain more (or fewer) modes such as 4^{th}, 5^{th}, 6^{th} and 7^{th}.

If the number of sensors to be used are not sufficient and optimal to represent the modes of interest for the structure with various crack lengths, then the selected signals are very hard to use for vibration-based SHM. Hence, one must ensure that the sensors are placed optimally despite the fact that not all vectors $\hat{\mathbf{\Phi}}_{\text{BL}}^{a\%}$, and $\hat{\mathbf{\Phi}}_{\text{BL}}^{b\%}$ are necessarily linearly independent. Thus, the EIDV methodology was generalized. A subset of the left singular vectors $\mathbf{U}_{\text{aug}}^{\text{EIDV}}$ of $\mathbf{\Phi}_{\text{aug}}^{\text{EIDV}}$ is used instead of the full augmented modal matrix

in Eq. (6). To select this subset, the singular values of $\mathbf{\Phi}_{\text{aug}}^{\text{EIDV}}$ are computed, and the left vectors corresponding to the largest singular values are selected.

Using the resulting matrix $\mathbf{U}_{\text{aug}}^{\text{EIDV}}$, the generalized EIDV algorithm for establishing locations for sensor placement can be summarized as follows.

(1) Calculate the BL modes for the healthy structure and cracked structures based on PROM (with crack lengths in a range of interest).

(2) Calculate the generalized $\mathbf{MAC}$ matrix using Eq. (5) and select sensitive modes for each crack length.

(3) Construct BL modes for the healthy and the cracked structures by selecting candidate measurement DOFs (by transforming PROM coordinates to physical coordinates) with the sensitive modes chosen at step (2).

(4) Construct the augmented BL modal matrix $\mathbf{\Phi}_{\text{aug}}^{\text{EIDV}}$ using Eq. (6).

(5) Apply singular value decomposition, and obtain the left singular vectors of $\mathbf{\Phi}_{\text{aug}}^{\text{EIDV}}$. Select the singular vectors $\mathbf{U}_{\text{aug}}^{\text{EIDV}}$ corresponding to the largest singular values.

(6) Calculate the Fisher information matrix given by $\mathbf{A} = \mathbf{U}_{\text{aug}}^{\text{EIDV}^{\text{T}}}\mathbf{U}_{\text{aug}}^{\text{EIDV}}$.

(7) Calculate the effective independence distribution vector, defined as the diagonal of the matrix $\mathbf{E} = \mathbf{U}_{\text{aug}}^{\text{EIDV}}\mathbf{A}^{-1}\mathbf{U}_{\text{aug}}^{\text{EIDV}^{\text{T}}}$.

The number of significant (or nontrivial) singular values of $\mathbf{\Phi}_{\text{aug}}^{\text{EIDV}}$ are indicative of the number of sensors needed for sensing and the generalized EIDV technique.

4.3 Over-Sampled Measurement Locations

There are several possible criteria to assess the suitability of the selected measurement locations. They include the modal assurance criterion, the modified modal assurance criterion, the singular value decomposition, the measured energy per mode, and the Fisher information matrix (Penny, et al. (1994)). Herein, the singular value decomposition is used to assess the suitability of selected measurement locations. The method simply evaluates the ratio of the largest to the smallest singular value of the BL modal matrix based on the measurement DOFs. If this ratio is close to unity, then the choice of measurement locations is good. In contrasts, the larger the ratio, the worst the choice of locations. Thus, if the ratio of the largest and smallest singular values of $\mathbf{U}_{\text{aug}}^{\text{EIDV}}$ with selected measurement DOFs is not close to 1.0, additional locations are likely necessary to guarantee linear independence of $\mathbf{U}_{\text{aug}}^{\text{EIDV}}$, especially in the presence of measurement noise.

Note that the number of selection points is dominated by the number of singular values of $\mathbf{\Phi}_{\text{aug}}^{\text{EIDV}}$ because the rank of the left singular vectors $\mathbf{U}_{\text{aug}}^{\text{EIDV}}$ (from $\mathbf{\Phi}_{\text{aug}}^{\text{EIDV}}$) which guarantees linear independence is same as the number of selected singular values. Thus, additionally selected measurement locations based on the modified EIDV techniques cannot be chosen based on linear independence. Assumption of that fact is that the most important DOFs which are additionally selected are the DOF nearest to the DOF already selected. For instance, consider that the size of the matrix $\mathbf{U}_{\text{aug}}^{\text{EIDV}}$ is 300×5, where 300×5 indicates the number of candidate DOFs and the number of

modes respectively. Consider also that number of modes (which is 5) is the same as the number of selected singular values. By using the modified EIDV technique, a maximum 5 measurement DOFs can be selected and the size of $\mathbf{U}_{\text{aug}}^{\text{EIDV}}$ (with the selected DOFs) is 5×5. However, if the ratio of the maximum and the minimum singular values for the final $\mathbf{U}_{\text{aug}}^{\text{EIDV}}$ (with the selected DOF) is not closed to 1.0, then the 5 selected measurement locations are not enough to guarantee linear independence of the final $\mathbf{U}_{\text{aug}}^{\text{EIDV}}$. Thus, a new technique to select additional measurement DOFs in addition to the ones selected based on singular values is necessary to guarantee that the final augmented modal matrix has linearly independent columns (and thus, the ratio of the maximum and the minimum singular values of the final $\mathbf{U}_{\text{aug}}^{\text{EIDV}}$ is close to 1.0.). The additional measurement locations are referred to as over-sampled measurement locations.

Herein, a new technique to select over-sampled measurement locations is proposed. Specifically, denote by $\mathbf{R}$ the left eigenvectors of $\mathbf{\Phi}_{\text{aug}}^{\text{EIDV}}$ which contain the remainder (unselected) DOFs, and denote by $\mathbf{S}$ the left eigenvectors of $\mathbf{\Phi}_{\text{aug}}^{\text{EIDV}}$ which contain the selected DOFs. After the generalized EIDV technique is executed, the $\mathbf{U}_{\text{aug}}^{\text{EIDV}}$ is divided into $\mathbf{S}$ and $\mathbf{R}$. The main idea is that $\mathbf{R}$ can be represented as a linear combination of the columns of $\mathbf{S}$ as follows,

$$\mathbf{R} = \mathbf{S}\mathbf{C}, \tag{7}$$

where $\mathbf{C}$ is coefficient matrix which can be calculated using Eq. (7). By managing the matrix $\mathbf{C}$, the most important DOF which should be added to previously selected DOF (based on the generalized EIDV) can be selected. This procedure is applied until the desired number of over-sampled measurement DOF is reached. Following is the specific procedure to select over-sampled measurement locations.

(1) The generalized EIDV technique is executed to select optimal measurement DOF by using $\mathbf{U}_{\text{aug}}^{\text{EIDV}}$ with all candidate DOFs.

(2) The $\mathbf{U}_{\text{aug}}^{\text{EIDV}}$ is divided into $\mathbf{R}$ and $\mathbf{S}$.

(3) The coefficient matrix $\mathbf{C}$ is calculated by using Eq. (7).

(4) The standard deviation of the entries in each row of the matrix $\mathbf{C}$ is computed.

(5) The DOF which corresponds to the minimum standard deviation (computed at step (4)) is selected as an additional DOF to measure.

(6) The additional DOF is added to $\mathbf{S}$, and omitted from $\mathbf{R}$.

(7) Steps (3) to (7) are repeated until the desired number of additional DOFs is reached.

5 Numerical Examples

5.1 HMMWV Models

In this section, we demonstrate the generalized EIDV techniques based on PROMs for a high mobility multipurpose wheeled vehicle (HMMWV) base frame with a crack.

Fig. 1 shows the finite element model along with the candidate measurement locations. Fig. 2 shows each substructure of the HMMWV frame used to construct PROMs. The reinforcement frames in the rear and the front are attached to the leftrails and rightrails. The reinforcement frames which are attached to the leftrails have thickness variations as shown in Table 1. The cross-member is considered to have a crack, as shown in Fig. 3. The crack length varies (across the cross-member component) from 3.03% to 36.36%. The CB-CMS method is applied for healthy substructures (the parts of the structure which do not have any variations). The MC-PROM method is implemented for the substructures with thickness variations. The BMA approach is implemented to approximate the BL modes of the cracked HMMWV frame.

To select the frequency range of interest, the sensitive BL modes are identified by using the generalized $\mathbf{MAC}$ matrix in Eq. (5). The crack lengths of interest are 24.24%, 30.30%, and 39.39%. Figures 4, 5, and 6 show the $\mathbf{MAC}$ matrices computed between the healthy and the cracked structure with 24.24%, 30.30%, and 39.39% crack length. For these cracked structures, the 30^{th} mode is the most sensitive compared to the healthy structure. Thus, the 30^{th} modes of the healthy and cracked structures are used to construct the augmented modal matrix $\mathbf{\Phi}_{\text{aug}}^{\text{EIDV}}$.

Next, the generalized EIDV technique is applied to obtain the optimal sensor locations. Figure 7 shows the best four sensor locations to capture the 30^{th} mode for the cases 1 and 2 of thickness variations. The BL mode shapes of the cracked structure are considered to be measured only at those four locations. The selected sensor locations are identical for each case of thickness variations. These results show that, for this structure, the optimal sensor locations are affected much more by the crack length than by the thickness variations. The ratio of the largest and the smallest singular values of the set of left singular vectors (only with the selected measurement DOFs represented in Fig. 7) are not very close to 1.0. For the cases 1 and 2 of thickness variations, the ratios are 1.41. Thus, additional over-sampled measurement locations are needed. For that, 6 additional over-sampled measurement DOFs can be selected by the algorithm for over-sampled measurement locations. Figures 8 and 9 show these 6 additional over-sampled locations along with the 4 optimal sensor locations based on the modified EIDV method. These figures show also the 10 optimal sensor locations obtained only from the modified EIDV method for the case 1 of thickness variation. The 10 sensor locations in Fig. 8 (from the over-sampled algorithm) are well distributed. In contrast, some of the measurement locations in Fig. 9 (from the modified EIDV only) are doubled selected. This result demonstrates that the additional measurement locations above and beyond the number of selected singular values cannot be selected well by the modified EIDV method. Figures 10 and 9 also show the 10 optimal measurement locations for the case 2 of thickness variation by using the over-sampled algorithm and the EIDV method respectively. The results are similar to the results of case 1 of thickness variation. Table 2 shows the ratio of the largest and the smallest singular values of $\mathbf{U}_{\text{aug}}^{\text{EIDV}}$ with 10 measurement DOFs selected by generalized EIDV, and with 10 measurement locations selected by the generalized EIDV and over-sampled algorithm. The ratio of $\mathbf{U}_{\text{aug}}^{\text{EIDV}}$ with selected DOFs by using the over-sampled algorithm is closer to 1.0 because those 10 measurement locations are well distributed.

5.2 Robust Signal Processing Based on a Monte-Carlo Technique

It is often desirable to select optimal and minimal sensor locations to capture the mode shapes of cracked structures. However, when the thickness of some components of the structure vary, the structural characteristics (especially mode shapes) are affected. Then, the optimal sensor locations may also be affected by the change in the mode shapes. That means that robust sensor locations are required to capture the mode shapes of the structures in the presence of thickness variations. Herein, a Monte-Carlo technique is applied to determine statistically optimal and robust sensor locations. To apply the Monte-Carlo technique, a large number of possible thickness variations are considered, and optimal sensor locations for the resulting mode shapes are obtained. To compute the mode shapes for each thickness variation, PROM techniques are applied. One of the main advantages of PROMs is that reanalysis (for each thickness variations) is almost 100 times faster because any parameter value in the parameter range can be easily applied (Hong, et al. (2010)).

The reinforcement frames in the rear and the front (which are attached to the leftrails) have thickness variations. For the Monte-Carlo technique, 400 separate cases of possible thickness variations are applied to these reinforcement frames. The 26^{th} through the 30^{th} modes are identified and selected as sensitive modes (based on $\mathbf{MAC}$ matrices obtained using Eq. (5)) and are used for sensor placement. The total number of modes for the augmented bilinear modal matrix in Eq. (6) is 20. Then, the optimal number of measurement locations are decided based on the selected number of singular value of $\mathbf{\Phi}_{\text{aug}}^{\text{EIDV}}$ for each case of thickness variation. For instance, if all columns of $\mathbf{\Phi}_{\text{aug}}^{\text{EIDV}}$ in Eq. (6) are linearly independent, then the selected number of singular values is 20. In contrast, if the columns of $\mathbf{\Phi}_{\text{aug}}^{\text{EIDV}}$ are not linearly independent, then the selected number of singular values is smaller than 20. During the Monte-Carlo simulations, 14 or 15 optimal measurement locations are selected for each case of thickness variation. Then, only four measurement points are selected for all cases of thickness variation. These four selected measurement locations are chosen to be the statistically optimal locations. Thus, they are the most robust when used to capture the BL modes of the cracked structures for any thickness variation (in the range of interest). Figure 12 shows the four statistically optimal measurement locations obtained. Figures 13 and 14 represent the distribution of optimal sensor locations chosen along the leftrail and the rightrail structure (i.e. along the x coordinate) for all cases of thickness variation.

6 Conclusions

Identifying structural inspection points or desired sensor locations for the purpose of vibration-based structural health monitoring is an important challenge for cracked structures because of the nonlinearity created by the crack opening and closing. A new concept of bilinear (BL) modes has been used to address this issue. The BL modes are obtained using linear analysis techniques, and can be used to obtain BL mode approximations. To alleviate high computational costs in design applications and to find statistical simulation results based on Monte-Carlo simulations, a reduced order modeling method based on Craig-Bampton component mode synthesis and multi-component parametric reduced-order models was used. A generalized modal assurance criterion has been developed and used to find the BL modes that are most sensitive

to the presence of a crack. Using the selected BL modes, an augmented BL modal matrix has been formed and used in an algorithm based on a modified effective independence distribution vector (EIDV) method to select optimal inspection points (or measurement locations). When the selected optimal measurement locations based on the generalized EIDV method are not enough to maintain the linear independence of the set of left singular vector, a novel over-sampled algorithm was applied to select additional measurement locations. Finally, the optimal set of measurement locations (for the cracked structure) was selected (by the generalized EIDV method and the over-sampled algorithm), and the measurement locations were assessed by the ratio of the largest and the smallest singular values of the set of the left singular vectors. To select robust sensor locations for any thickness variation in a range of interest, a Monte-Carlo technique was implemented based on PROMs to select statistically optimal measurement locations. 400 cases of possible thickness variations were considered for a HMMWV frame, and 4 statistically optimal and robust measurement locations were selected. These four points are robust and statistically optimal to capture the mode shapes of the cracked HMMWV structure.

Acknowledgements

This work was partially supported by the Automotive Research Center, a U.S. Army RDECOM center of excellence for modeling and simulation of ground vehicles led by the University of Michigan.
UNCLASSIFIED: Dist A. Approved for public release.

References

Farhad Ansari, (2007), 'Practical Implementation of Optical Fiber Sensors in Civil Structural Health Monitoring', *Journal of Intelligent Material Systems and Structures*, Vol. 18, pp.879–889

E.B. Flynn and M.D. Todd, (2009), 'Optimal Placement of Piezoelectric Actuators and Sensors for Detecting Damage in Plate Strucures', *Journal of Intelligent Material Systems and Structures*, Vol. 21, pp.265–274

M. Krommer, M. Zellhofer and K.-H. Heilbrunner, (2009), 'Strain-type Sensor Networks for Structural Monitoring of Beam-type Structures', *Journal of Intelligent Material Systems and Structures*, Vol. 20, pp.1875–1888

Daniel C. Kammer, (1991), 'Sensor Placement for On-Orbit Modal Identification and Correlation of Large Space Structures', *Journal of Guidance*, Vol. 14(2), pp.251–259

J.E.T. Penny, M.I. Friswell and S.D. Garvey, (1994), 'Automatic Choice of Measurement Locations for Dynamic Testing', *AIAA Journal*, Vol. 32(2), pp.407–414

W.C. Hurty, (1965), 'Dynamic Analysis of Structural Systems using Component Modes', *AIAA Journal*, Vol. 3(4), pp.678–685

R.R. Craig Jr. and M.C.C. Bampton, (1968), 'Coupling of Substructures for Dynamic Analyses', *AIAA Journal*, Vol. 6(7), pp.1313–1319

S. Rubin, (1975), 'Improved Component-Mode Representation for Structural Dynamic Analysis', *AIAA Journal*, Vol. 13(8), pp.995–1006

R.M. Hintz, (1975), 'Improved Component-Mode Representation for Structural Dynamic Analysis', *AIAA Journal*, Vol. 13(8), pp.1007–1016

R.R. Craig Jr. and C.J. Chang, (1976), 'Free Interface Methods of Structure Coupling for Dynamic Analysis', *AIAA Journal*, Vol. 14(11), pp.1633–1635

E. Balmes, (1996), 'Parametric Families of Reduced Finite Element Modes: Theory and Application', *Mechanical Systems and Signal Processing*, Vol. 10(4), pp.381–394

E. Balmes, F. Ravary and D. Langlais,, (2004), 'Uncertainty Propagation in Modal Analysis', *in Proceedings of IMAC-XXII: A Conference and Exposition on Structural Dynamics*, Dearborn, MI, IMAC-XXII-57.

G. Zhang, M.P. Castanier and C. Pierre, (2005), 'Integration of Component-Based and Parametric Reduced-Order Modeling Methods for Probabilistic Vibration Analysis and Design', *in Proceedings of the Sixth European Conference on Structural Dynamics*, Paris, France, pp.993–998.

K. Park, (2008), 'Component-Based Vibration Modeling Methods for Fast Re-Analysis and Design of Complex Structures', Doctoral Dissertation, University of Michigan

S.-K. Hong, B.I. Epureanu, M.P. Castanier, and D J. Gorsich, (2010), 'Parametric Reduced-Order Models for Predicting the Vibration Response of Complex Structures with Component Damage and Uncertainties', *Journal of Sound and Vibration*, doi: 10.1016/j.jsv.2010.09.022

O. Poudou and C. Pierre, (2003), 'Hybrid Frequency-Time Domain Methods for the Analysis of Complex Structural Systems with Dry Friction Damping', *in Proceedings of the 44th AIAA/ASME/ASCE/AHS/ASC Structures, Structural Dynamics and Materials Conference*, Norfolk, VA.

O. Poudou, (2004), 'A New Hybrid Frequency-Time Domain Method for the Forced Vibration of Elastic Structures with Friction and Intermittent Contact', *in Proceedings of the 10th International Symposium on Transport Phenomena and Dynamics of Rotating Machinery*, Honolulu, Hi.

A. Saito, M.P. Castanier, C. Pierre and O. Poudou, (2009), 'Efficient Nonlinear Vibration Analysis of the Forced Response of Rotating Cracked Blades', *Journal of Computational and Nonlinear Dynamics*, Vol. 4, pp.011005-1–011005-10

M. Chati, R. Rand and S. Mukherjee, (1997), 'Modal Analysis of a Cracked Beam', *Journal of Sound and Vibration*, Vol. 207, pp.249–270

A. Saito, M.P. Castanier and C. Pierre, (2009), 'Estimation and Veering Analysis of Nonlinear Resonant Frequencies of Cracked Plates', *Journal of Sound and Vibration*, Vol. 326(3–5), pp.725–739

A. Saito and B.I. Epureanu, (2010), 'Bilinear Modal Representations for Reduced-Order Modeling of Localized Piecewise-Linear Oscillators', *Journal of Sound and Vibration*, submitted

R.J. Allemang and D.L. Brown, (1982), 'A Correlation Coefficient for Modal Vector Analysis', *in Proceedings of the International Modal Analysis Conference*, pp.110–116.

R.J. Allemang, (2010), 'The Modal Assurance Criterion - Twenty Years of Use and Abuse', *Sound and Vibration*, Vol. 37(8), pp.14–23

List of Tables

1 Thickness variations in substructures 15
2 The ratio of the largest and the smallest singular value 15

Table 1 Thickness variations in substructures

Substructure	Case 1	Case 2
L_{rear}	3.038 mm $\rightarrow 5.562$ mm	3.038 mm $\rightarrow 4.114$ mm
L_{front}	3.038 mm $\rightarrow 4.991$ mm	3.038 mm $\rightarrow 3.552$ mm

Table 2 The ratio of the largest and the smallest singular value

Case	Type of selection method	Ratio for singular value
1	Over-sampled	1.04148356006958
	Modified EIDV	1.1975357311883
2	Over-sampled	1.02422819735424
	Modified EIDV	1.2123994255097

List of Figures

1 Finite element model for a HMMWV frame 17
2 Substructuring of the HMMWV frame 17
3 Substructure for the cracked cross-member frame 17
4 **MAC** between modes for healthy HMMWV and the structure with 24.24% crack 18
5 **MAC** between modes for healthy HMMWV and the structure with 30.30% crack 18
6 **MAC** between modes for healthy HMMWV and the structure with 39.39% crack 18
7 4 optimal sensor locations based on the 30^{th} mode by using modified EIDV method for case 1 and 2 of thickness variations 19
8 10 optimal sensor locations based on the 30^{th} mode by using modified EIDV method and over-sampled algorithm for the case 1 of thickness variations 19
9 10 optimal sensor locations based on the 30^{th} mode by using modified EIDV method for the case 1 of thickness variations 19
10 10 optimal sensor locations based on the 30^{th} mode by using modified EIDV method and over-sampled algorithm for the case 2 of thickness variations 19
11 10 optimal sensor locations based on the 30^{th} mode by using modified EIDV method for the case 2 of thickness variations 20
12 Statistically optimal sensor locations for 400 cases of thickness variations 20
13 Optimal sensor locations distribution of leftrail frame structure for all cases of thickness variation 20
14 Optimal sensor locations distribution of rightrail frame structure for all cases of thickness variation 21

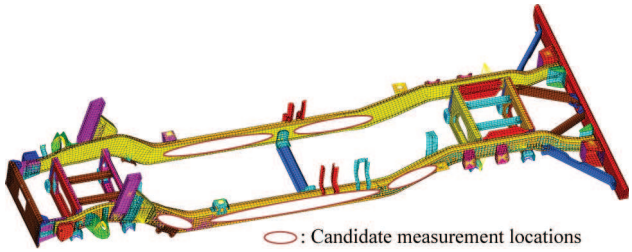

Figure 1 Finite element model for a HMMWV frame

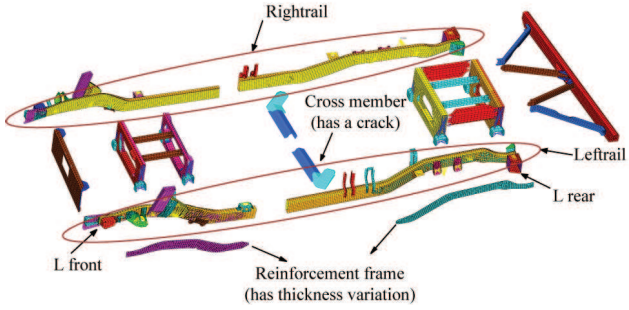

Figure 2 Substructuring of the HMMWV frame

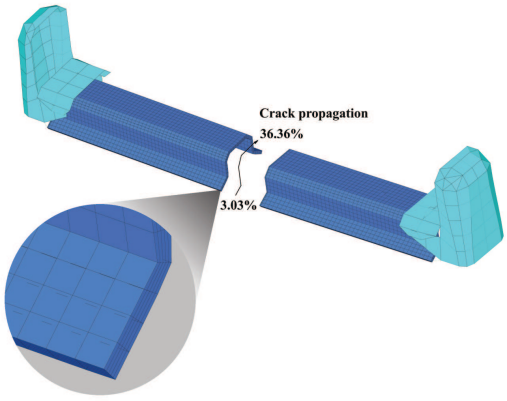

Figure 3 Substructure for the cracked cross-member frame

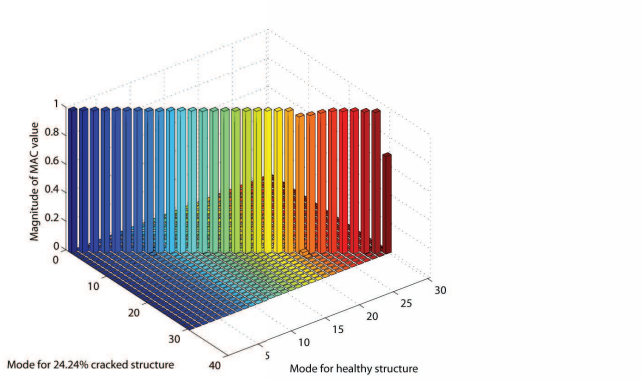

Figure 4 **MAC** between modes for healthy HMMWV and the structure with 24.24% crack

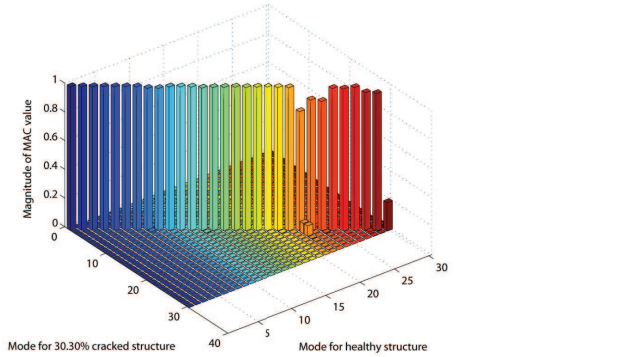

Figure 5 **MAC** between modes for healthy HMMWV and the structure with 30.30% crack

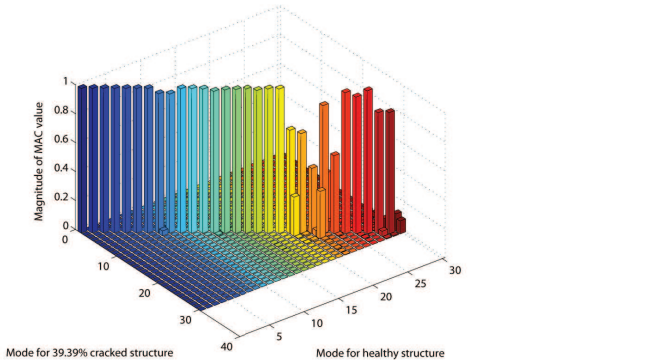

Figure 6 **MAC** between modes for healthy HMMWV and the structure with 39.39% crack

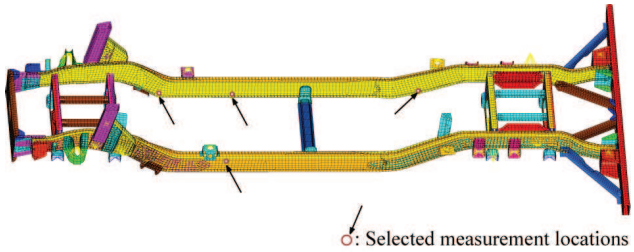

Figure 7 4 optimal sensor locations based on the 30^{th} mode by using modified EIDV method for case 1 and 2 of thickness variations

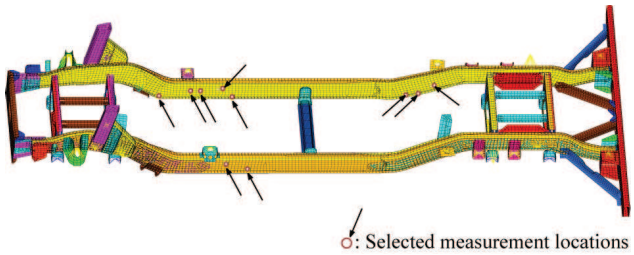

Figure 8 10 optimal sensor locations based on the 30^{th} mode by using modified EIDV method and over-sampled algorithm for the case 1 of thickness variations

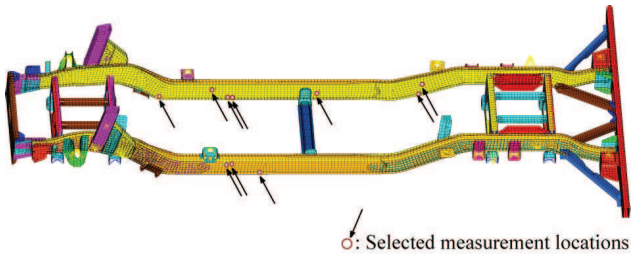

Figure 9 10 optimal sensor locations based on the 30^{th} mode by using modified EIDV method for the case 1 of thickness variations

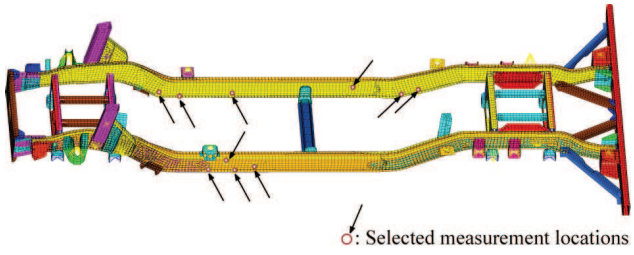

Figure 10 10 optimal sensor locations based on the 30^{th} mode by using modified EIDV method and over-sampled algorithm for the case 2 of thickness variations

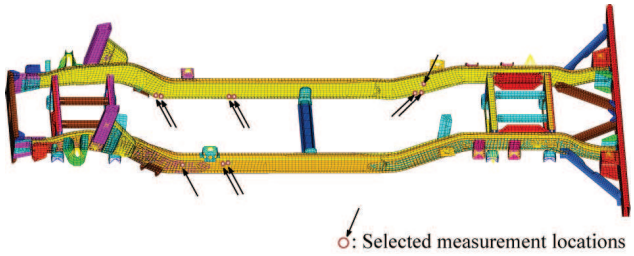

Figure 11 10 optimal sensor locations based on the 30^{th} mode by using modified EIDV method for the case 2 of thickness variations

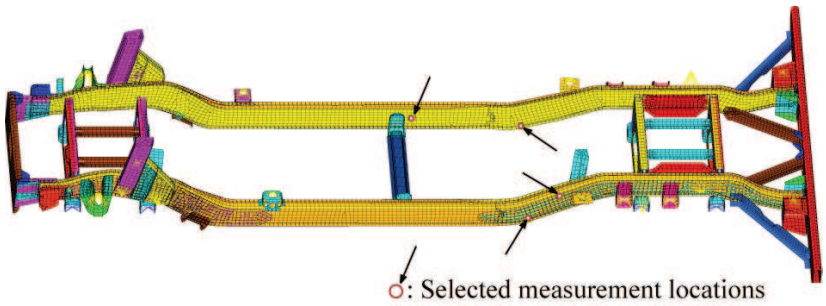

Figure 12 Statistically optimal sensor locations for 400 cases of thickness variations

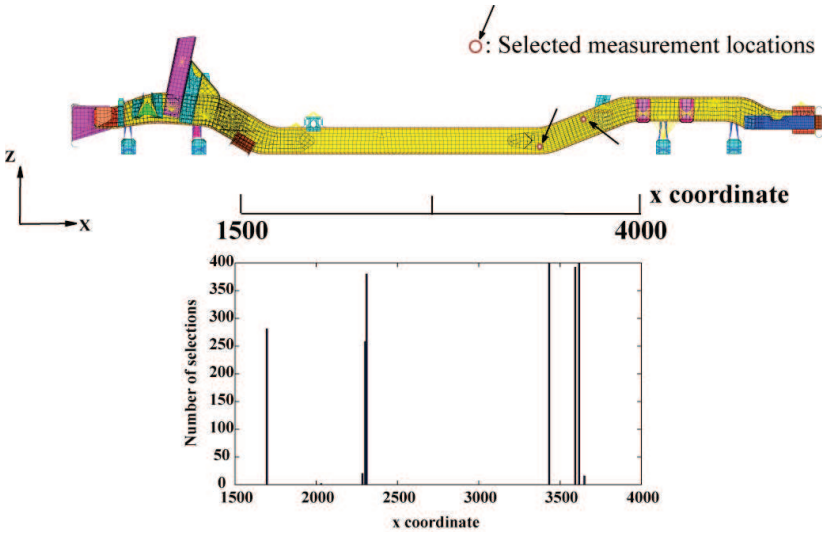

Figure 13 Optimal sensor locations distribution of leftrail frame structure for all cases of thickness variation

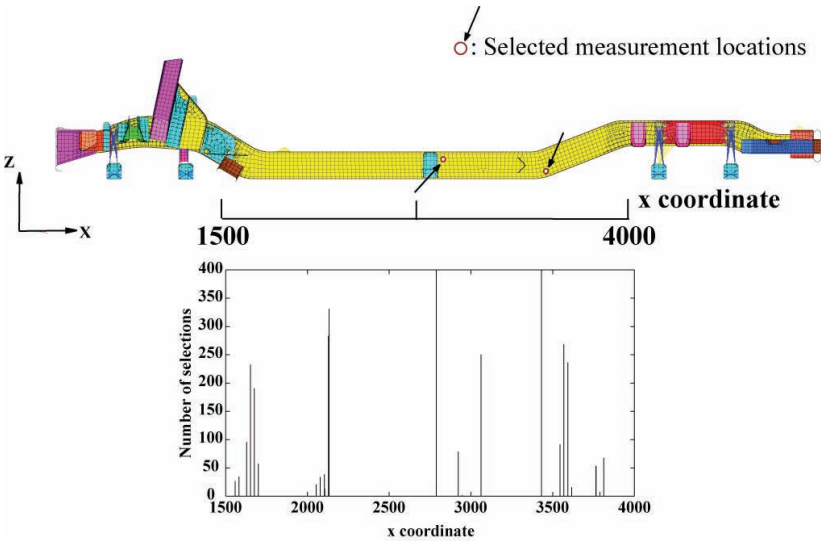

Figure 14 Optimal sensor locations distribution of rightrail frame structure for all cases of thickness variation